Supplementary Figures

Androgens inhibit protective $CD8^+$ T cell responses against pre-erythrocytic malaria parasites

Duncombe *et al.*

1. Supplementary Tables 1 – 2
2. Supplementary Figures 1 – 11

Supplementary Tables

Parasite strain	Mouse strain	Sporozoite attenuation strategy	Biological Sex	Ref
P. yoelii (17XNL), *P. berghei* (ANKA)	BALB/c	RAS, CPS-CN	Female	1
P. yoelii (265BY)	BALB/c; 129P2Sv/ev	RAS, CPS-CQ, CPS-PQ	Female (BALB/c); Sex not reported (129P2Sv/ev)	2
P. yoelii (17XNL), *P. berghei* (NK65)	BALB/c; C57BL/6; Swiss Webster	RAS, CPS-PQ	Sex not reported	3
P. yoelii (17XNL)	BALB/c; Swiss Webster	GAP ΔSAP1	Female	4
P. yoelii (17XNL)	BALB/c	GAP ΔSAP1	Female	5
P. yoelii (17XNL), P. yoelii (YM), P. berghei	BALB/c; C57BL/6; Swiss Webster	GAP ΔSAP1, GAP ΔFABB/F, RAS	Sex not reported	6
P. yoelii (17XNL)	BALB/c	GAP ΔUIS3, GAP ΔUIS4	Female	7
P. yoelii (17XNL)	BALB/c;C.129S7(B6)	GAP ΔUIS3, GAP ΔUIS4	Female	8
P. yoelii (265 BY), *P. berghei* (ANKA)	BALB/c; C57BL/6	GAP Δp36p, RAS	Sex not reported	9
P. berghei (ANKA)	BALB/c; C57BL/6	GAP Δp36p, RAS	Female	10
P. berghei (ANKA)	C57BL/6	GAP ΔUIS3, GAP Δp36p, RAS, CPS-PQ, CPS-AZ, CPS-CQ, CPS-PYR	Female	11
P. berghei (ANKA)	C57BL/6	RAS, CPD-CQ	Sex not reported	12
P. berghei (ANKA)	C57BL/6	GAP ΔSLARP	Female	13
P. yoelii (17XNL), P. berghei (ANKA)	BALB/c; C57BL/6	CPS-PQ	Sex not reported	14
P. berghei (ANKA)	BALB/c; C57BL/6	CPS-CN	Female	15
P. berghei (NK65)	C57BL/6	GAP ΔPKG	Female	16
P. berghei (ANKA)	C57BL/6; μMT	CPS-AZ, CPS-CM	Female	17

Supplementary Table 1: Was mouse sex listed in key papers about mouse sporozoite vaccines?

References from Nganou-Makamdop and Sauerwein[18] with respect to whether or not biological sex of the mice were noted by reviewed paper.

1 Purcell, L. A. *et al.* Chemically attenuated *Plasmodium* sporozoites induce specific immune responses, sterile immunity and cross-protection against heterologous challenge. *Vaccine* **26**, 4880-4884, doi:10.1016/j.vaccine.2008.07.017 (2008).

2 Belnoue, E. *et al.* Protective T cell immunity against malaria liver stage after vaccination with live sporozoites under chloroquine treatment. *J Immunol* **172**, 2487-2495, doi:10.4049/jimmunol.172.4.2487 (2004).

3 Schmidt, N. W., Butler, N. S., Badovinac, V. P. & Harty, J. T. Extreme CD8 T cell requirements for anti-malarial liver-stage immunity following immunization with radiation attenuated sporozoites. *PLoS Pathog* **6**, e1000998, doi:10.1371/journal.ppat.1000998 (2010).
4 Aly, A. S., Lindner, S. E., MacKellar, D. C., Peng, X. & Kappe, S. H. SAP1 is a critical post-transcriptional regulator of infectivity in malaria parasite sporozoite stages. *Mol Microbiol* **79**, 929-939, doi:10.1111/j.1365-2958.2010.07497.x (2011).
5 Aly, A. S. *et al.* Targeted deletion of SAP1 abolishes the expression of infectivity factors necessary for successful malaria parasite liver infection. *Mol Microbiol* **69**, 152-163, doi:10.1111/j.1365-2958.2008.06271.x (2008).
6 Butler, N. S. *et al.* Superior antimalarial immunity after vaccination with late liver stage-arresting genetically attenuated parasites. *Cell Host Microbe* **9**, 451-462, doi:10.1016/j.chom.2011.05.008 (2011).
7 Tarun, A. S. *et al.* Protracted sterile protection with *Plasmodium* yoelii pre-erythrocytic genetically attenuated parasite malaria vaccines is independent of significant liver-stage persistence and is mediated by CD8+ T cells. *J Infect Dis* **196**, 608-616, doi:10.1086/519742 (2007).
8 Trimnell, A. *et al.* Genetically attenuated parasite vaccines induce contact-dependent CD8+ T cell killing of *Plasmodium* yoelii liver stage-infected hepatocytes. *J Immunol* **183**, 5870-5878, doi:10.4049/jimmunol.0900302 (2009).
9 Douradinha, B. *et al.* Genetically attenuated P36p-deficient *Plasmodium berghei* sporozoites confer long-lasting and partial cross-species protection. *Int J Parasitol* **37**, 1511-1519, doi:10.1016/j.ijpara.2007.05.005 (2007).
10 van Dijk, M. R. *et al.* Genetically attenuated, P36p-deficient malarial sporozoites induce protective immunity and apoptosis of infected liver cells. *Proc Natl Acad Sci U S A* **102**, 12194-12199, doi:10.1073/pnas.0500925102 (2005).
11 Friesen, J. & Matuschewski, K. Comparative efficacy of pre-erythrocytic whole organism vaccine strategies against the malaria parasite. *Vaccine* **29**, 7002-7008, doi:10.1016/j.vaccine.2011.07.034 (2011).
12 Nganou-Makamdop, K., van Gemert, G. J., Arens, T., Hermsen, C. C. & Sauerwein, R. W. Long term protection after immunization with *P. berghei* sporozoites correlates with sustained IFNgamma responses of hepatic CD8+ memory T cells. *PLoS One* **7**, e36508, doi:10.1371/journal.pone.0036508 (2012).
13 Silvie, O., Goetz, K. & Matuschewski, K. A sporozoite asparagine-rich protein controls initiation of *Plasmodium* liver stage development. *PLoS Pathog* **4**, e1000086, doi:10.1371/journal.ppat.1000086 (2008).
14 Putrianti, E. D., Silvie, O., Kordes, M., Borrmann, S. & Matuschewski, K. Vaccine-like immunity against malaria by repeated causal-prophylactic treatment of liver-stage *Plasmodium* parasites. *J Infect Dis* **199**, 899-903, doi:10.1086/597121 (2009).
15 Purcell, L. A., Yanow, S. K., Lee, M., Spithill, T. W. & Rodriguez, A. Chemical attenuation of *Plasmodium berghei* sporozoites induces sterile immunity in mice. *Infect Immun* **76**, 1193-1199, doi:10.1128/IAI.01399-07 (2008).
16 Falae, A. *et al.* Role of *Plasmodium berghei* cGMP-dependent protein kinase in late liver stage development. *J Biol Chem* **285**, 3282-3288, doi:10.1074/jbc.M109.070367 (2010).

17 Friesen, J. *et al.* Natural immunization against malaria: causal prophylaxis with antibiotics. *Sci Transl Med* **2**, 40ra49, doi:10.1126/scitranslmed.3001058 (2010).
18 Nganou-Makamdop, K. & Sauerwein, R. W. Liver or blood-stage arrest during malaria sporozoite immunization: the later the better? *Trends Parasitol* **29**, 304-310, doi:10.1016/j.pt.2013.03.008 (2013).

Marker	Fluorochrome	Clone	Source	Catalog	Titer (in 50 µL MM)
Live/Dead	Zombie yellow		Biolegend		1:250
CD3E	BUV395	145-2C11	BD Bioscience	563565	1 µL
B220	BV711	RA3-6B2	Biolegend	103255	0.25µL
CD4	BB700	GK1.5	BD Bioscience	745922	0.5µL
CD8a	APC-H7	53-6.7	BD Bioscience	560182	0.5µL
CD44	BUV737	IM7	BD Bioscience	612799	0.5µL
CD62L	PE-CY7	MEL-14	BD Bioscience	560516	0.5µL
CD69	BV786	H1-2F3	BD Bioscience	564683	1µL
CXCR3	BV650	CXCR3-173	BD Bioscience	740630	1µL
PD1	PE/DAZZLE594	29F.1A12	Biolegend	135228	0.5µL
LAG3	BB515	C9B7W	BD Bioscience	564672	0.5µL
TCF1	BV421	S33-966	BD Bioscience	566692	1µL
CD107a	PE	1D4B	BD Bioscience	558661	0.5µl (in 200µL MM)
IFNg	BV421	XMG1.2	Biolegend	505830	1µL
TNF	FITC	MP6-XT22	BD Bioscience	554418	1µL
Granzyme B	AF647	GB11	BD Bioscience	560212	0.5µL
CSP-tetramer	APC		NIH tetramer facility		1µL

Supplementary Table 2: Flow cytometry antibody manifest.

Supplementary Figures

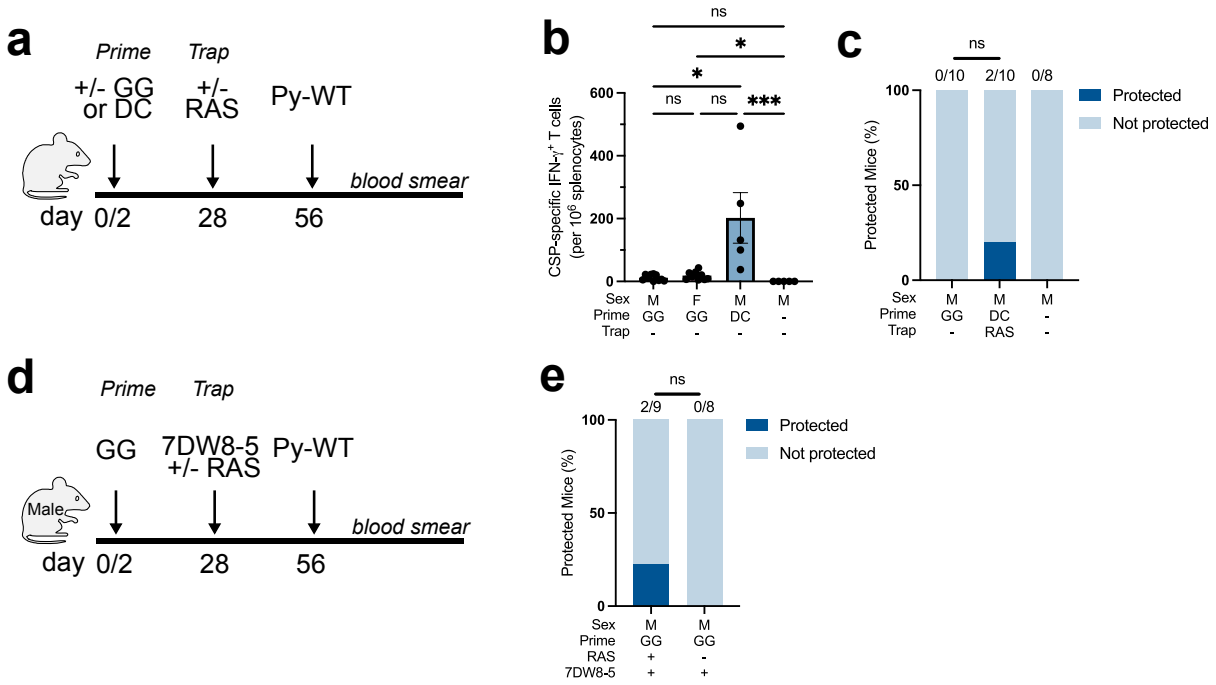

Supplementary Figure 1: Enhancing P&T vaccination does not increase protection in male BALB/cJ mice. a. Male and female BALB/cJ mice were vaccinated with gene gun (GG) CSP DNA vaccination alone or left as naïve mice or primed with CSP peptide-pulsed dendritic cells (DC) followed by $2x10^4$ radiation attenuated sporozoites (RAS), or remained naïve to RAS. **b.** CSP-specific IFN-γ^+ T cells in the spleen by ELISPOT on samples collected 28 days following priming steps. Data shown are from 1-2 independent experiments (n = 5-10/group). **c.** Percentages of mice protected against challenge with $1x10^3$ Py-WT sporozoites by blood smears through 14 days post-challenge. Data shown are from 2 independent experiments (n = 8-10/group) **d.** P&T vaccination with the addition of the glycolipid adjuvant 7DW8-5 to the RAS trapping step or adjuvant by itself. **e.** Percentages of mice protected against challenge with $1x10^3$ Py-WT sporozoites by blood smears through 14 days post-challenge. Data are shown from 2 independent experiments (n= 8-9/group). Statistical significance for data in **c** and **e** was determined by a two-sided Fisher exact test. Only relevant comparisons are shown. Statistical significance for data in **b** was determined by the Kruskal-Wallis test with Dunn's multiple comparison. Error bars represents mean ± s.e.m; ***p<0.001, **p<0.01, *p<0.05, ns p>0.05. Source data are provided as a Source Data file.

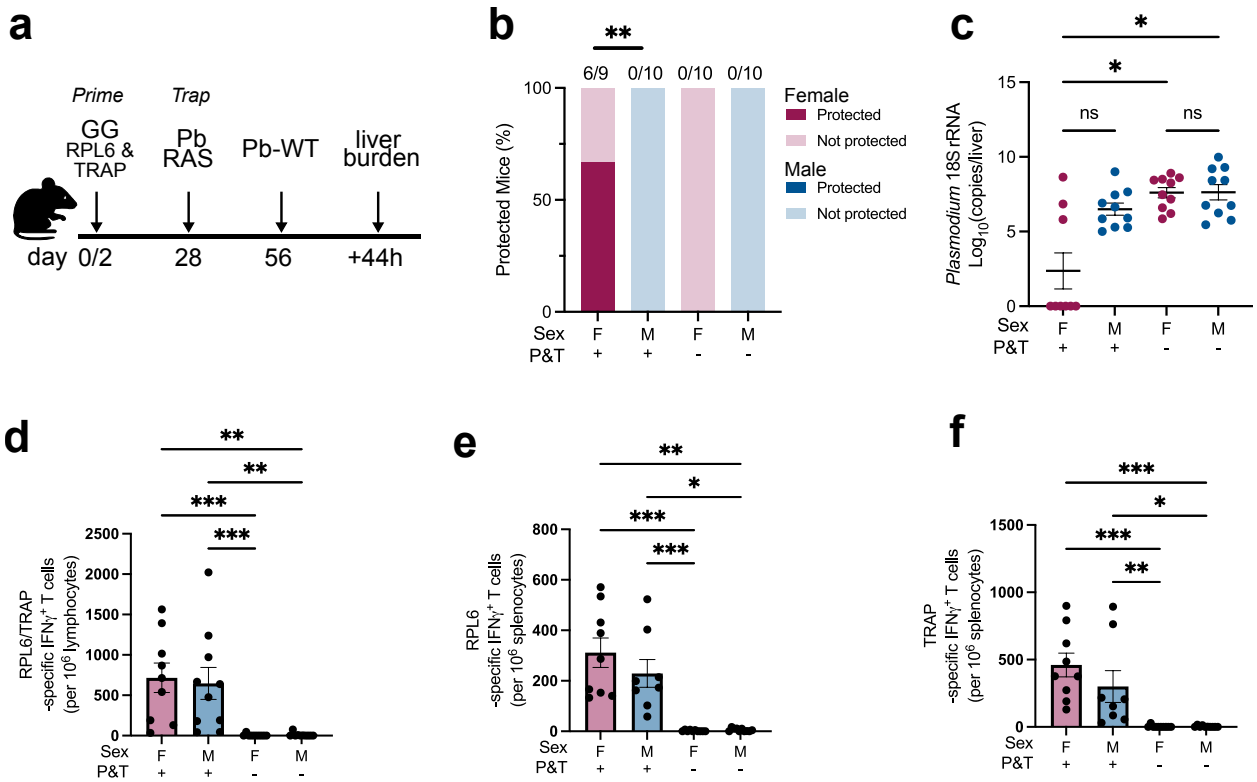

Supplementary Figure 2: Prime-and-trap malaria vaccination induces sex-specific protection against sporozoite challenge in a *Plasmodium berghei* and C57BL/6 rodent malaria model. a. Scheme of male (M) and female (F) C57BL/6 mice prime-and-trap (P&T) vaccination experiment. **b.** Protection following 1x10^3 Py-WT sporozoite challenge defined as no detectable pan-*Plasmodium* 18S rRNA copies 44 hours post-challenge. **c.** Liver burden as absolute pan-*Plasmodium* 18S rRNA copy numbers 44 hr post-challenge. **d - f.** Liver and spleen were harvested from the mice at the 44 hours post-challenge timepoint and IFN-γ ELISPOT was performed in the presence of either RPL6 peptide (**e**), TRAP peptide (**f**), or both (**d**). IFN-γ spot forming units (SFU) are shown per million liver (**d**) and spleen (**e - f**) lymphocytes for each mouse normalized to the corresponding media control. Data from 2 independent experiments (n= 8-10/group). Statistical significance for data in **b** was determined by a two-sided Fisher exact test. Only relevant comparisons are shown. Statistical significance for data in **c - f** was determined by the Kruskal-Wallis test with Dunn's multiple comparison. Error bars represents mean ± s.e.m; ***p<0.001, **p<0.01, *p<0.05, ns p>0.05. Source data are provided as a Source Data file.

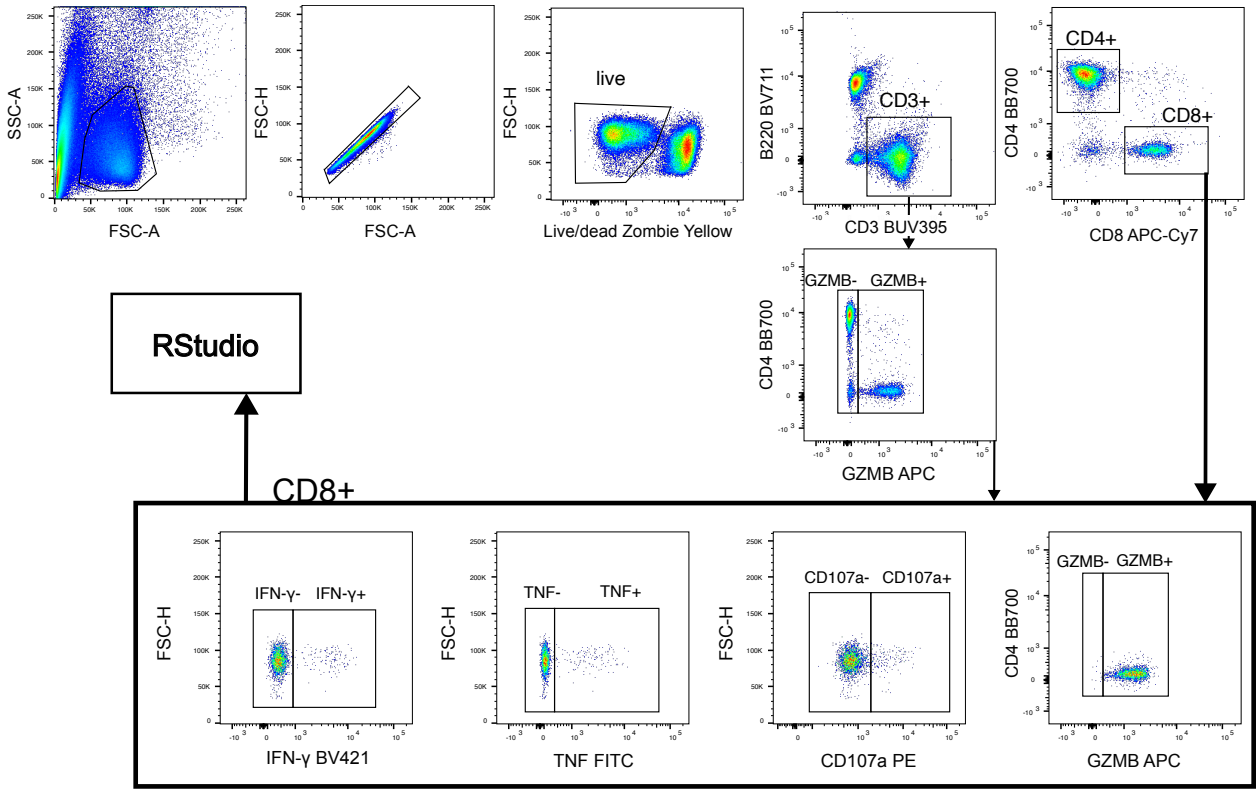

Supplementary Figure 3. Gating strategy for T cell Intracellular Cytokine Staining. Data in Figures 2b-i, 4d-i, and 6 were obtained using a 9-color multiparameter flow cytometry panel following intracellular cytokine staining (ICS). Events were selected using a lymphocyte gate, then a singlet event gate, and then a live/dead stain. CD3 and B220 were next used to identify T cells and exclude B cells. $CD3^+$ cells were subsequently evaluated for either granzyme B (GZMB) or for CD4 and CD8. $CD8^+$ cells were further chracterized for expression of IFN-γ, TNF, and the CD107a degranulation marker. Further downstream heiracheal and boolean gating was performed in RStudio.

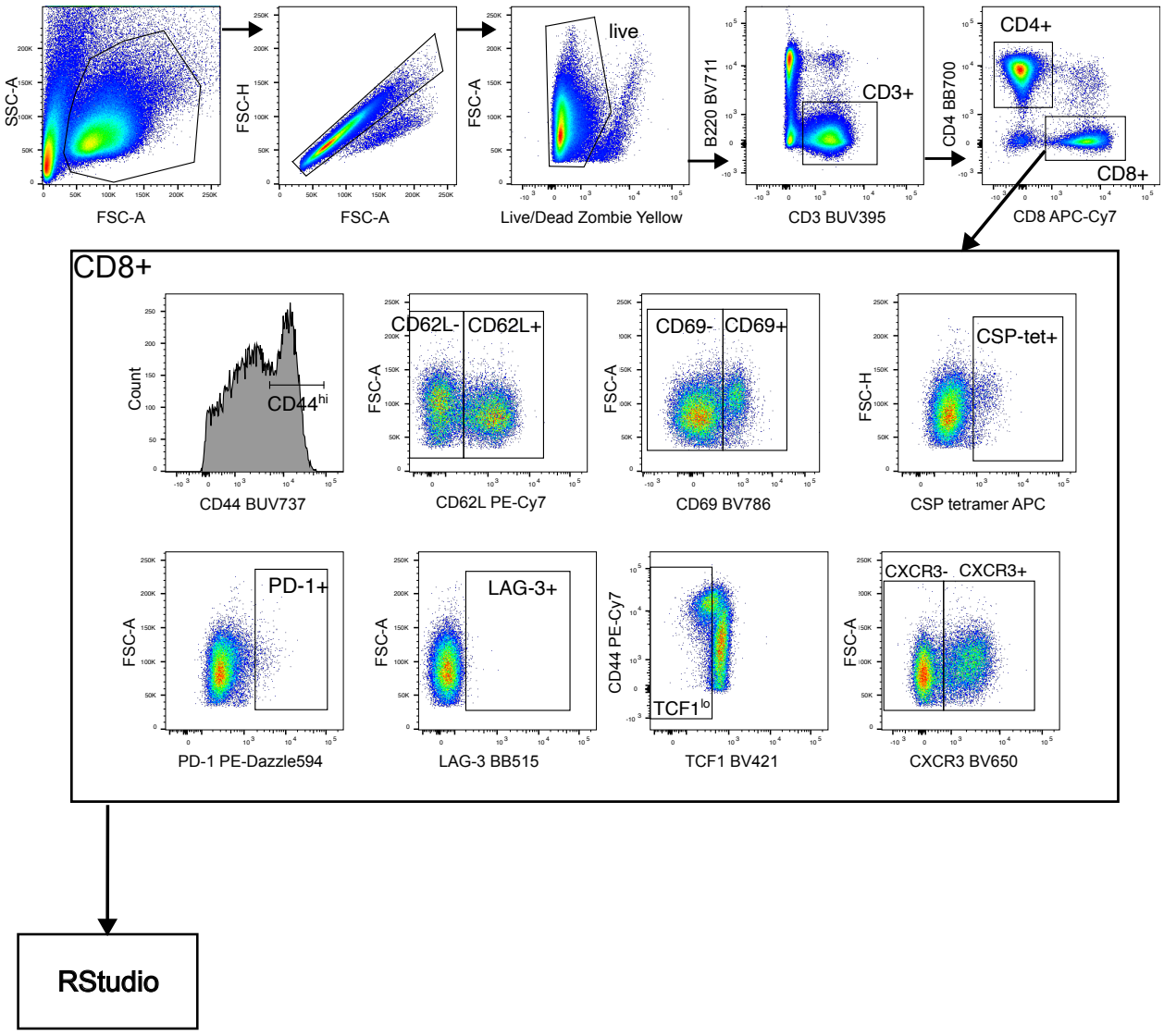

Supplementary Figure 4. Gating strategy for T cell flow cytometry.
Data presented in Figures 2 (j-l), and 4 (j-m) were obtained using a 13-color multiparameter flow cytometry panel. Events were selected using a lymphocyte gate, then a singlet event gate, and then a live/dead stain. CD3 and B220 were next used to identify T cells and exclude B cells. $CD3^+$ cells were gated for CD4 and CD8 co-receptor expression. For $CD8^+$ populations, cell were further characterized for expression of CD44, CD62L, CD69, CSP-tetramer, LAG-3, PD-1, TCF1, and CXCR3. Further downstream heiracheal gating was performed in RStudio.

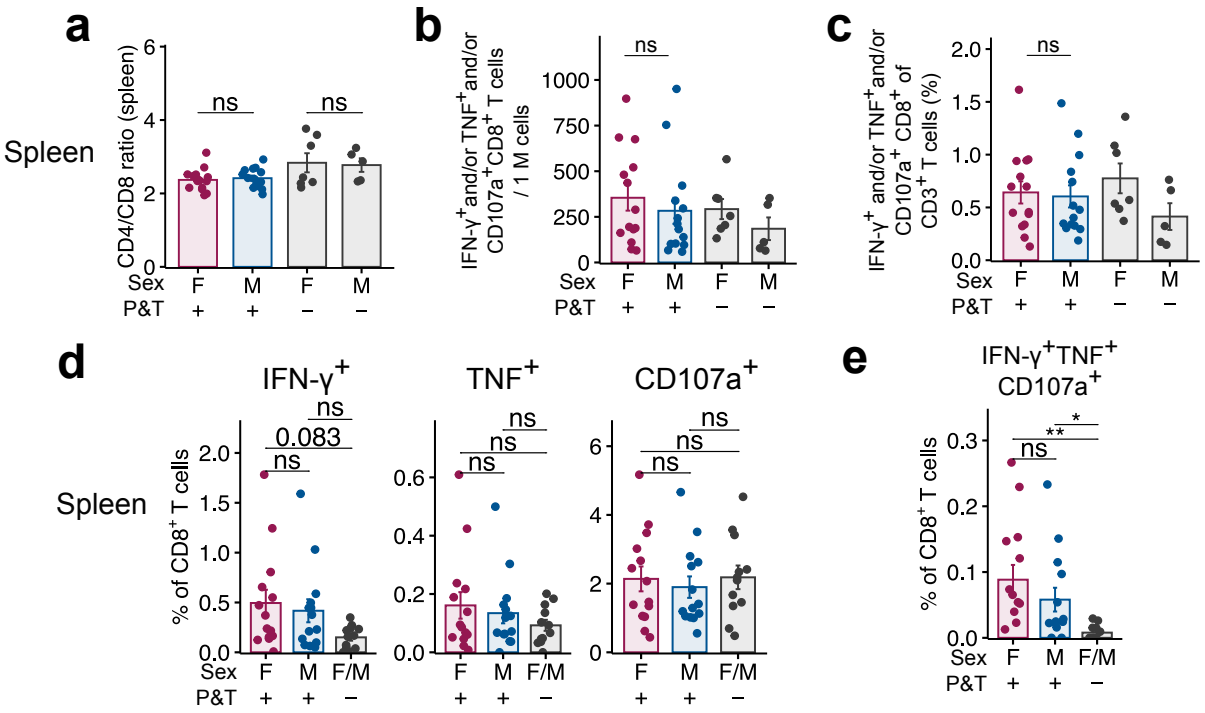

Supplementary Figure 5: Evaluation of vaccine-induced CD8⁺ T cells in the spleen between males and females. Female and male BALB/cJ mice were vaccinated with the prime-and-trap (P&T) regimen. 28 days later, spleen cells were analyzed by flow cytometry. **a.** Ratio of CD4-to-CD8 T cells in the spleen of P&T vaccinated (+) and unvaccinated mice (-) female (F) and male (M) BALB/cJ mice. **b - c.** Quantification of total CSP^{280}-specific CD8⁺ T cells as total number of IFN-γ⁺ and/or TNF⁺ and/or CD107a⁺ producing CD8⁺ T cells per million splenocytes (**b**) and as a proportion of CD3⁺ splenic T cells (**c**). **d - e.** Quantification of proportion of IFN-γ⁺ (**d** - left), TNF⁺ (**d** - middle), CD107a⁺ (**d** - right) and IFN-γ⁺TNF⁺CD107a⁺ (**e**) producing CD8⁺ T cells in the spleen. Data are shown from 3 independent experiments (n = 14 for P&T groups, n= 5-7 unvaccinated group per sex). Statistical significance for data was determined by Kruskal-Wallis tests with Dunn's multiple comparison; Error bars are mean ± s.e.m. **p<0.01, *p<0.05, ns p>0.05. Source data are provided as a Source Data file.

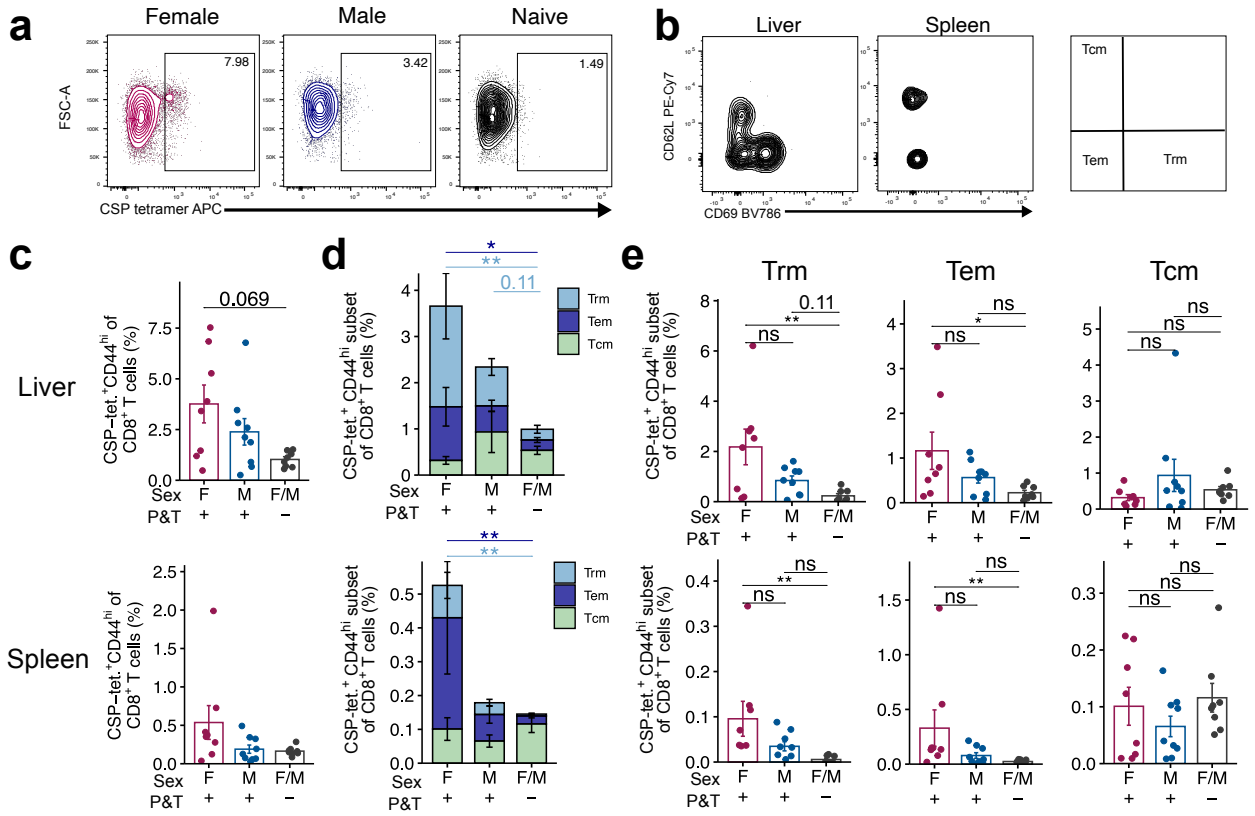

Supplementary Figure 6: Extended evaluation of sex differences in CD8⁺ T cells memory subsets. a. Representative flow cytometry plot (gated on CD8⁺ T cells) depicting H-2K^{d}-PyCSP$^{280-288}$ tetramer positive (CSP-tet.$^{+}$) cells isolated from the liver of P&T vaccinated (+) female (F - left) and male (M - middle) mice and an unvaccinated (-) control mouse (right) collected 28 days after the last immunization. **b.** Representative flow cytometry plot depicting CSP-tetramer^{+}CD44^{hi} CD8^{+} T cells Trm, Tem, and Trm phenotypes. Gating calculations performed in R. See supplementary Figure S4 for gating tree. **c.** Frequency of CSP-tetramer^{+}CD44^{hi} cells of CD8^{+} T cells in livers (top) and spleens (bottom). **d - e.** Frequency of CSP tetramer^{+}CD44^{hi} memory subsets, Trm (CD62L^{-}CD69^{+} ; left), Tem (CD62L^{-}CD69^{+}; middle), and Tcm (CD62L^{+}CD69^{-}; right) of total CD8^{+} T cell in livers (top – also depicted in Figure 2k) and spleens (bottom). Data are shown from 2 independent experiments (n= 8-9). Statistical significance for data was determined by Kruskal-Wallis test with Dunn's multiple comparison. In **d,** individual p-values for significant differences are shown, colored to correspond to memory T cell subsets where relevant; Error bars represents mean ± s.e.m. **p<0.01, *p<0.05, ns p>0.05. Source data are provided as a Source Data file.

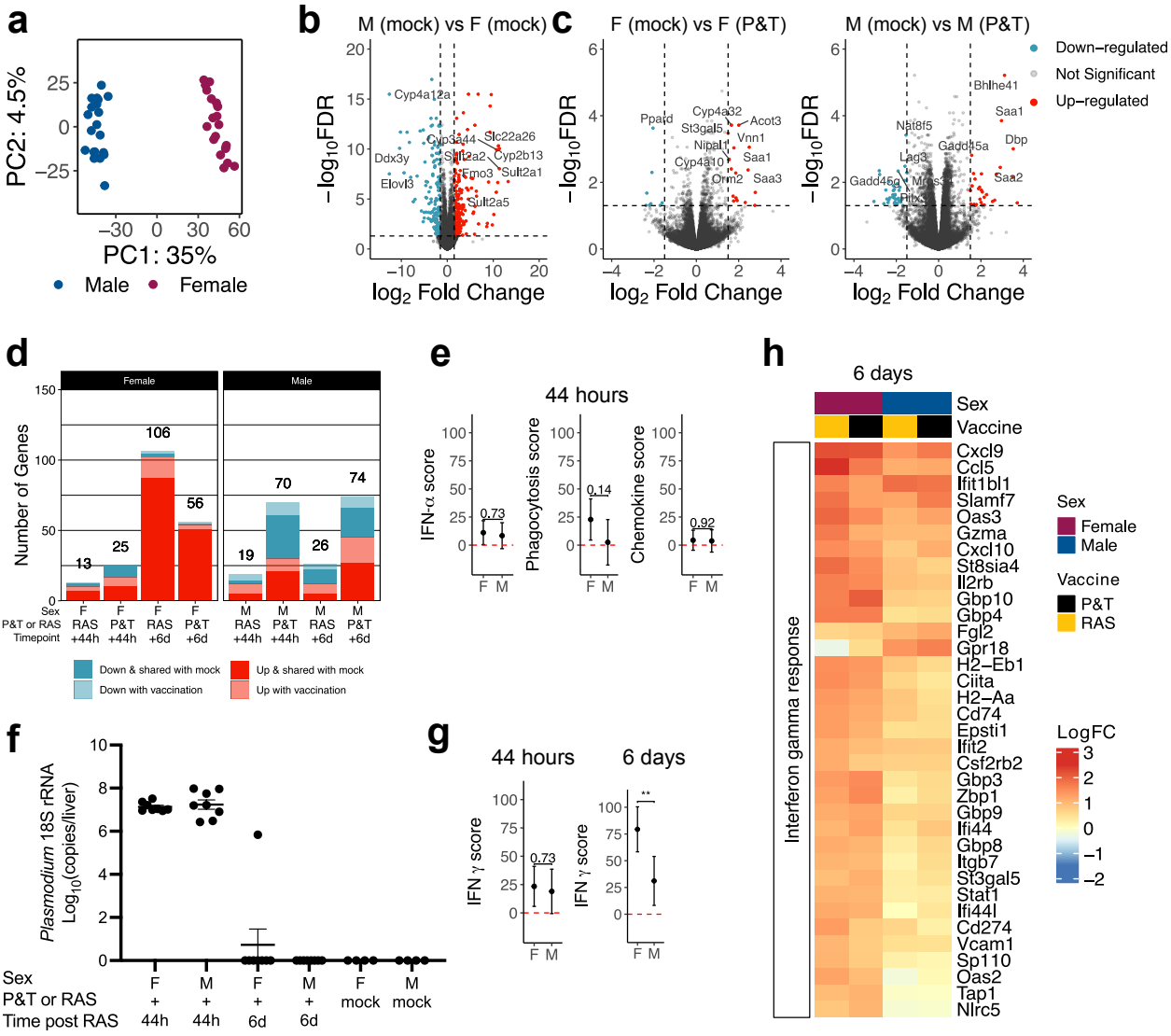

Supplementary Figure 7: Male mice experience a restricted inflammatory response compared to females after Radiation Attenuated Sporozoite (RAS) immunization (extended). **a.** Principal Component (PC) plot after exclusion of sex-chromosome-linked genes of male and female transcriptomes following RAS immunization. **b - c.** Volcano plot of differentially expressed genes between mock-injected male (M) and female (F) mice (**b**), P&T vaccinated female and mock females (**c -** left), and P&T vaccinated males and mock-injected males (**c –** right). Red indicates genes up-regulated in female and blue indicates genes down-regulated relative to male mock (**b, c** - right**)** to female mock (**c** – left) with FDR < 0.05 and |LogFC| > 1.5, Benjamini-Hochberg (BH) adjusted. The top ten most significant differentially expressed genes are depicted. **d.** Depiction of number of differentially expressed genes for each comparison (FDR < 0.05 and |LogFC| > 1.5, BH adjusted). Dark blue and dark red indicate down-regulated and up-regulated genes that are unique to the response to sporozoites respectively. Light blue and light red indicate genes that are also differentially expressed between mock male and female mice. **e.** Pathway score of aggregate samples by interferon (IFN) alpha response, phagocytosis, and response to

chemokines pathways at 44 hours post-immunization (n = 8/group) relative to mock samples (n = 4/group). **f.** Livers dissected for RNAseq were processed for *Plasmodium* 18S rRNA reverse transcription polymerase chain reaction (RT-PCR) to measure parasite burden. Data are shown as absolute 18S rRNA $\log_{10}$ copy numbers per liver. **g.** Pathway score of aggregate samples by IFN-γ pathways at 44 hours (left) and 6 days (right) post-immunization (n = 8 per group) relative to mock samples (n = 4). **h.** Heatmap and hierarchal clustering of genes that contain at least one differentially expressed gene at the 6 day timepoint (FDR <0.05, |LogFC| > 1, BH adjusted) and appear in the Hallmark 'Interferon gamma response'. Column annotations depict biological sex and vaccine status. Data produced from 1 independent replicate (n = 4/group). Error bars in **e** and **g** represent the mean value with 95% confidence intervals. **p<0.01, *p<0.05, ns p>0.05.

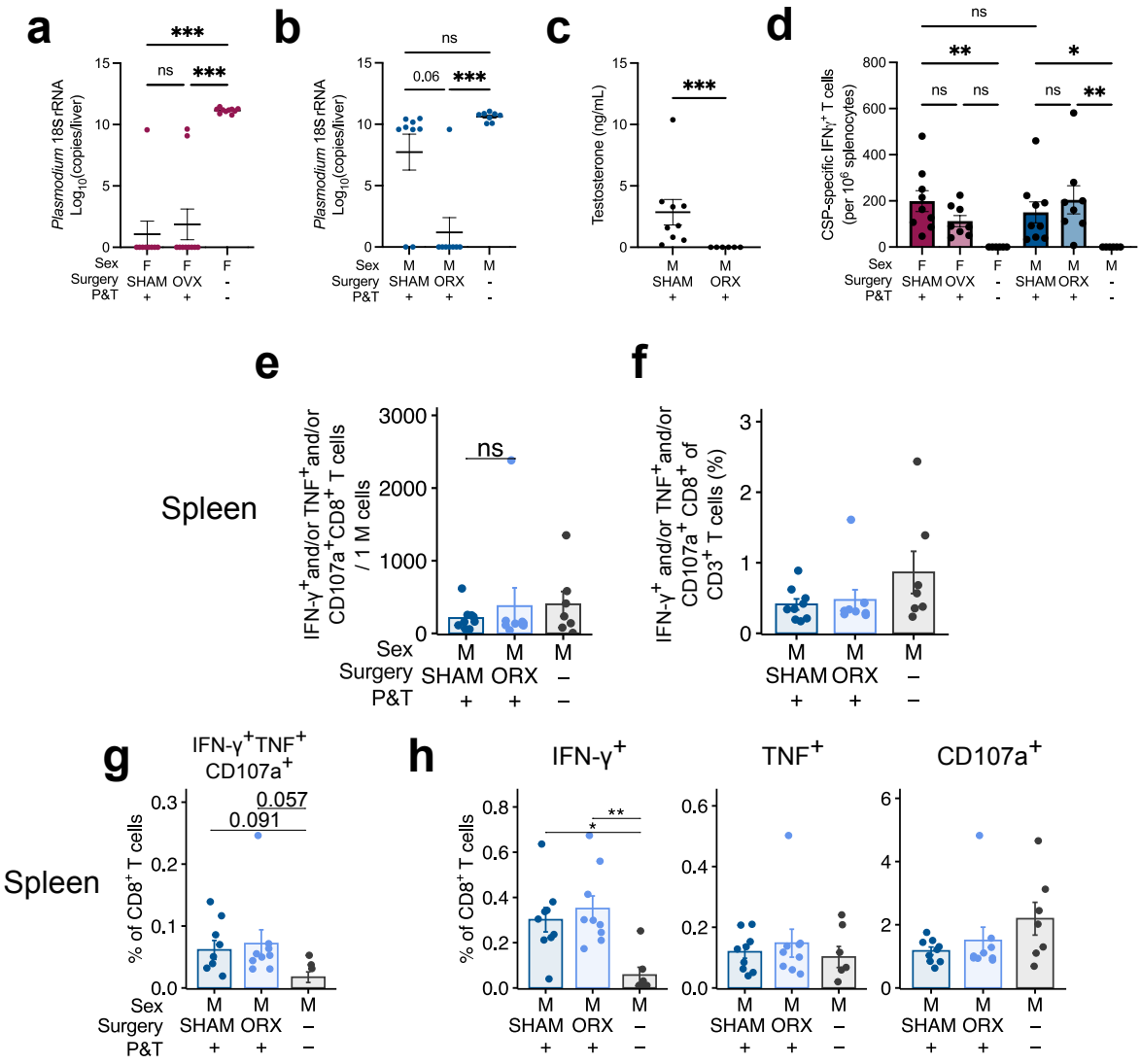

Supplementary Figure 8: Further evaluation of the impact of ORX and OVX on splenic CD8⁺ T cells. a - b. Liver burden values from Figure 4b-c as absolute pan-*Plasmodium* 18S rRNA copy numbers 44 hr post-challenge. Data are shown from 2 independent experiments (n = 8 - 10/group). **c.** Confirmatory testosterone measurements in serum by ELISA of a subset of mice in Figure 4c. **d.** Spleens were harvested from a subset of the mice in Figure 4a-c at the 44 hours post-challenge timepoint and IFN-γ ELISPOT was performed in the presence of $CSP^{280-288}$ peptide**.** IFN-γ spot forming units (SFU) are shown per million splenocytes for each mouse normalized to the corresponding media control. Data are shown from 2 independent experiments (n = 6-9/group). **e - f.** ICS quantification of total CSP responsive CD8⁺ T cells as total IFN-γ⁺ and/or TNF⁺ and/or CD107a⁺ producing CD8⁺ T cells per million splenocytes (**e**) and as proportion of splenic CD3⁺ T cells (**f**). **g - h.** Quantification of proportion of IFN-γ⁺TNF⁺CD107a⁺ (**g**) and IFN-γ⁺ (**h** - left), TNF⁺ (**h** - middle), CD107a⁺ (**h** - right) producing CD8⁺ T cells in the spleen. Data for **e - h** are shown from 2 independent experiments (n = 7-9/group). Statistical significance for data in **a - b, d,** and **e - h** was determined by Kruskal-Wallis test with Dunn's multiple comparison and data

in **c** was evaluated with a two-sided Wilcoxon Test; Error bars are mean ± s.e.m. ***p<0.001, **p<0.01, *p<0.05, ns p>0.05. Source data are provided as a Source Data file.

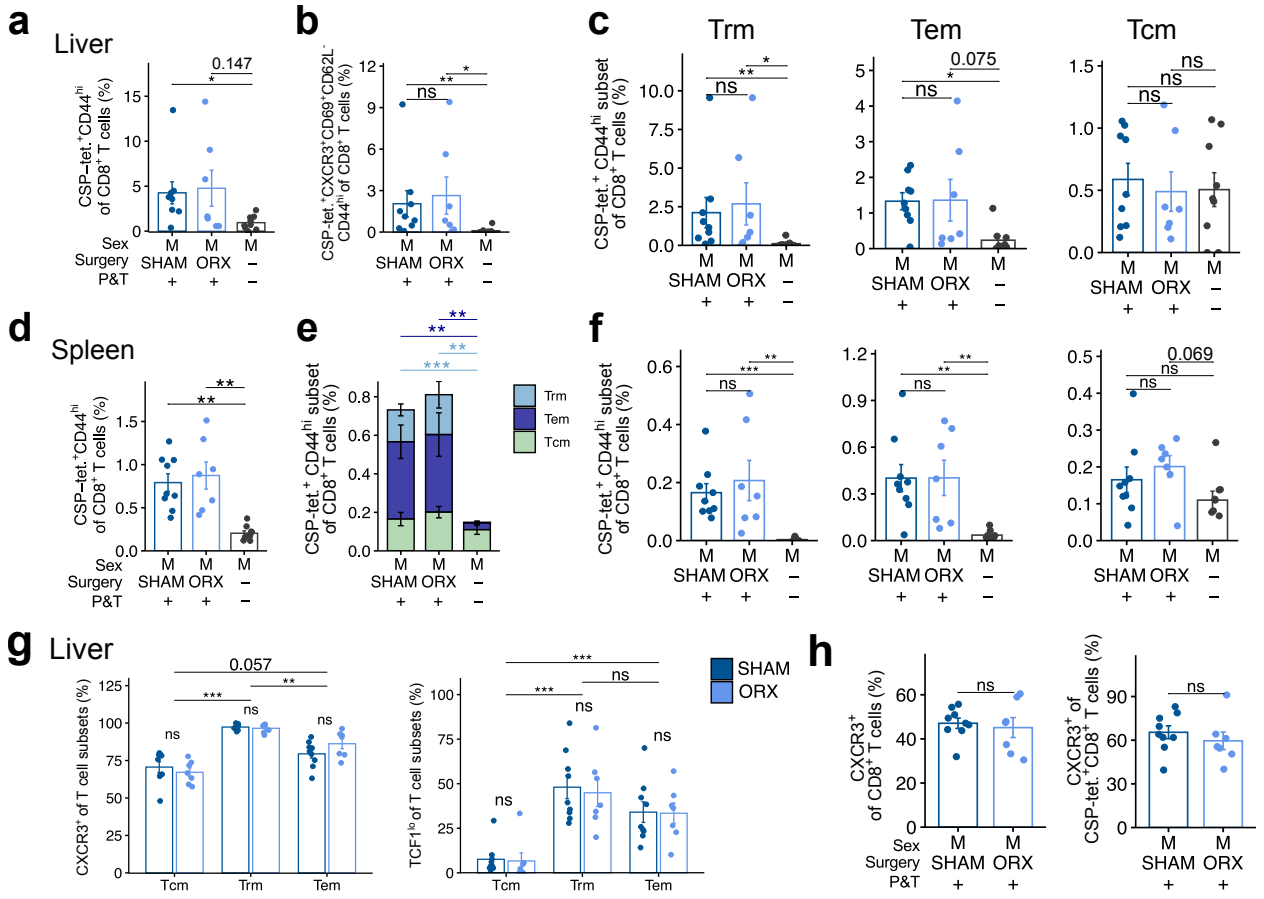

Supplementary Figure 9: Further evaluation of impact of ORX on CD8⁺ T cell fate in male mice. ORX- or SHAM-operated male BALB/cJ mice were vaccinated (+) by the primer-and-trap (P&T) regimen or left naïve (-). 28 days later, liver and spleen lymphocytes were analyzed by flow cytometry. **a** and **d.** Frequency of CSP-tetramer⁺CD44^{hi} cells of CD8⁺ T cells in the liver (**a**) and the spleen (**d**). **b - c** and **e - f.** Frequency of CSP tetramer⁺CD44^{hi} Trm (CXCR3⁺CD62L⁻CD69⁺- **b;** CD62L⁻CD69⁺- **c** and **f**), Tem (CD62L⁻CD69⁺), Tcm (CD62L⁺CD69⁻) subsets of total CD8⁺ T cell in the liver (**b - c**) and spleen (**e - f**). **g.** Quantitative evaluation of proportion of CXCR3⁺ (left) and TCF1^{lo} (right) on CSP-tetramer⁺CD44^{hi} CD8 T cells phenotypically defined as Trm, Tem, and Tcm cells in the liver**. h.** Proportion of CXCR3⁺ on CD8⁺ T cells (left) and CSP-tetramer⁺CD8⁺ T cells (right). Data are shown from 2 independent experiments (n = 7-9/group). Statistical significance for data in **a - f** and between T cell memory phenotypes in **g** was determined by Kruskal-Wallis tests with Dunn's multiple comparison. Data in **h** and between SHAM and ORX male within a T cell memory phenotype in **g** was evaluated with two-sided Wilcoxon Test; ***p<0.001, **p<0.01, *p<0.05, ns p>0.05. Source data are provided as a Source Data file.

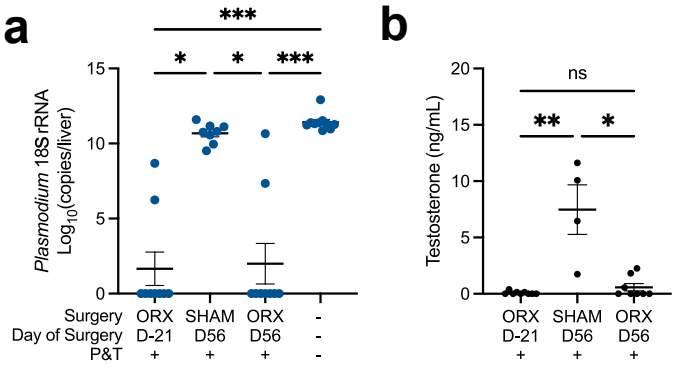

Supplementary Figure 10: Protection of male mice depends on hormone environment at time of challenge (extended). a. Liver burden values from **Figure 5b** as absolute pan-*Plasmodium* 18S rRNA copy numbers 44 hr post-challenge. Data are shown from 2 independent experiments (n= 8-10/group). **b.** Confirmatory testosterone measurements in serum by ELISA of a subset of mice in Figure 5b. Only relevant comparisons are shown. Statistical significance for data was determined by the Kruskal-Wallis test with Dunn's multiple comparison. Error bars represents mean ± s.e.m; ***p<0.001, **p<0.01, *p<0.05, ns p>0.05. Source data are provided as a Source Data file.

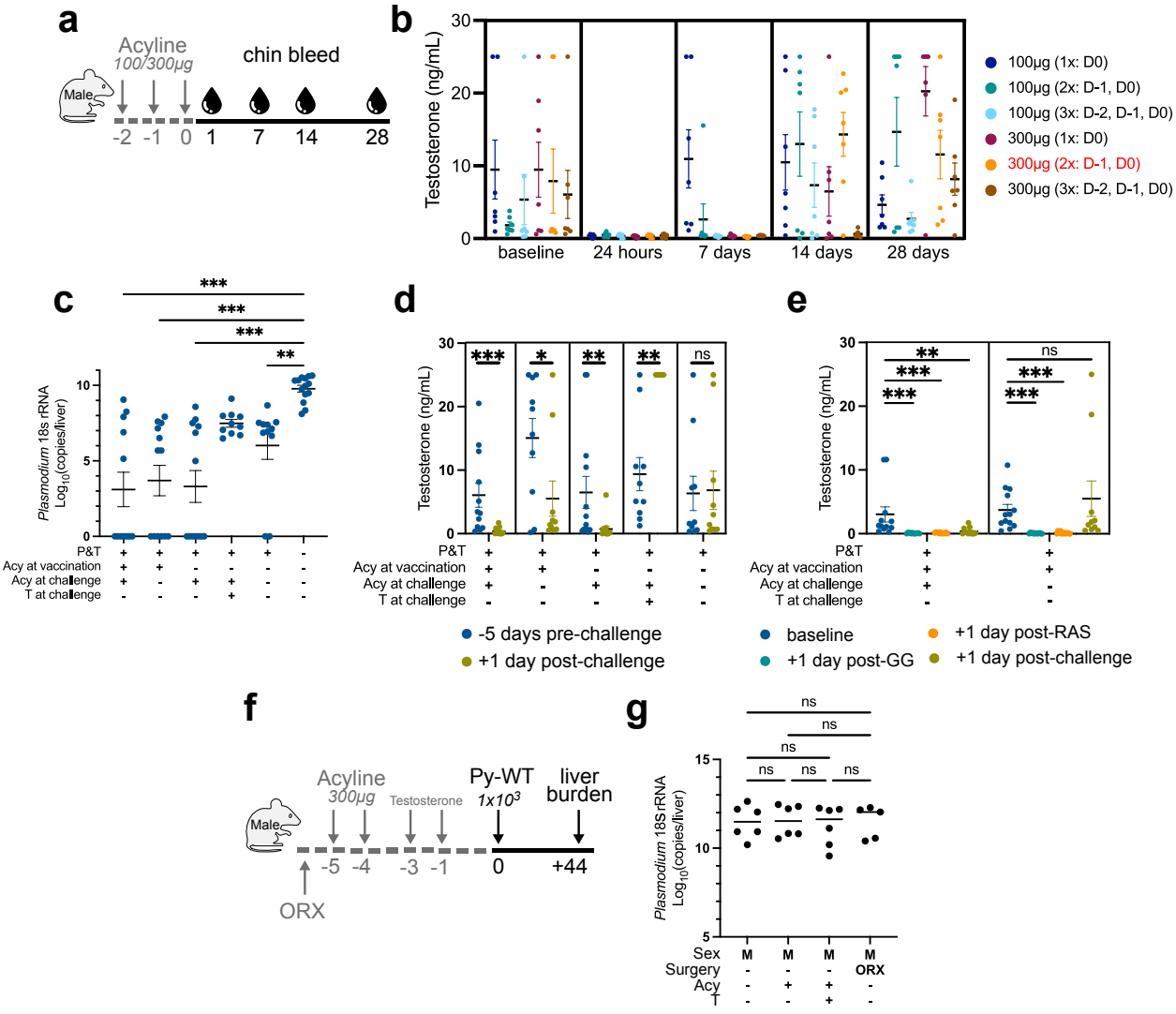

Supplementary Figure 11: Acyline as a model for acute, reversible reduction of testosterone levels. a - b. Male mice received one or multiple doses of 100µg or 300µg Acyline and were monitored for testosterone levels measured by ELISA up to 28 days post last dose (2 independent replicates, n = 7/group). **c.** Liver burden values from Figure 5d as absolute pan-*Plasmodium* 18S rRNA copy numbers 44 hr post-challenge. **d-e** Confirmatory testosterone measurements by ELISA of the mice in Figure 5d. **f.** Male mice either were orchiectomized (ORX), received Acyline and/or testosterone, or left untreated, then challenged with 1000 Py-WT spz (2 - 3 independent replicates, n = 10 - 13/group). **g.** Liver burden as absolute pan-*Plasmodium* 18S rRNA copy numbers 44 hr post-challenge (2 independent replicates, n = 5 - 6/group). No statistical test was conducted for **b** due to an observatory readout. Statistical significance for data in **c, e,** and **g** was determined by the Kruskal-Wallis test with Dunn's multiple comparison; data in **d** was determined by a paired two-sided Wilcoxon Test. Error bars represent mean ± s.e.m; ***p<0.001, **p<0.01, *p<0.05, ns p>0.05. Source data are provided as a Source Data file.